Nanoscale Assembly of Enantiomeric Supramolecular Gels Driven by the Nature of Solvents

Tómas A. Gudmundsson,[a,b] Geethanjali Kuppadakkath,[a] Dipankar Ghosh,[a] Manuel Ruether,[b] Annela Seddon,[c] Rebecca E. Ginesi,[d] James Doutch,[e] Dave J. Adams,[d] Thorfinnur Gunnlaugsson,[b] and Krishna K. Damodaran*[a]

a. Department of Chemistry, Science Institute, University of Iceland, Dunhagi 3, 107 Reykjavík, Iceland
b. School of Chemistry and Trinity Biomedical Sciences Institute (TBSI) and Advanced Materials and BioEngineering Research (AMBER) Centre, Trinity College Dublin, The University of Dublin, Dublin 2, D02 PN40, Ireland.
c. School of Physics, HH Wills Physics Laboratory, Tyndall Avenue, University of Bristol, Bristol, BS8 1TL, UK.
d. School of Chemistry, University of Glasgow, Glasgow, G12 8QQ, UK.
e. ISIS Pulsed Neutron and Muon Source, Harwell Science and Innovation Campus, Didcot, OX11 0QX, UK.

Contents

1. Circular Dichroism (CD) experiments

Solution state samples were prepared by dissolving the gelator to obtain a concentration of 0.02 wt/v%. The data was collected using a Jasco J-1100 CD spectrometer with 50 nm/min continuous scanning over 300 – 200 nm at 25.0 °C with 10 accumulations.

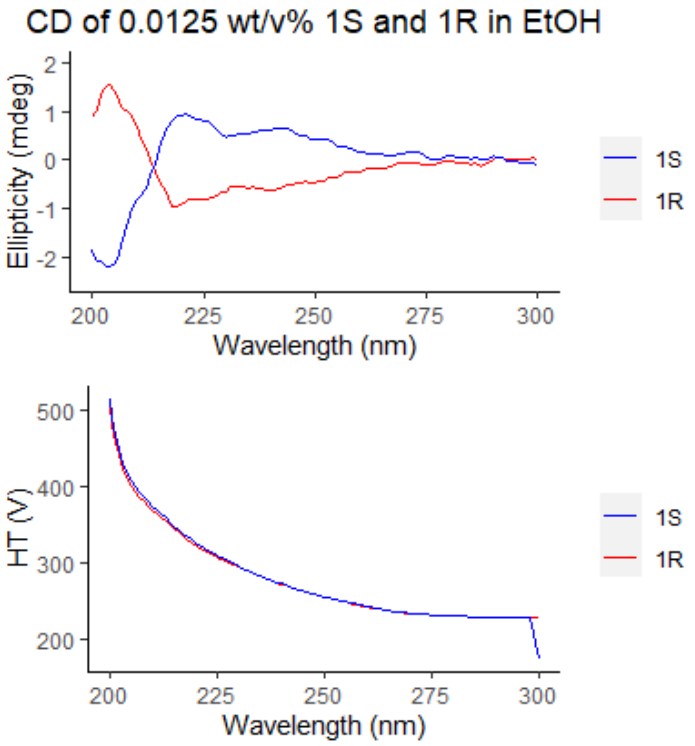

Figure S1. CD spectra of the solutions of **1R** and **1S** at 0.0125 wt/v% in EtOH (top) and the corresponding HT voltage graph (bottom).

We were unable to collect data with non-polar aromatic solvents or aqueous solutions of DMF and DMSO due to the high UV cut-off point. The CD signal of **1R** displayed a positive and a negative maximum at ~210 and 240 nm, respectively, which can be attributed to the π–π stacking of the aromatic moieties. The CD spectrum of **1S** was found to be nearly the mirror image of **1R**, showing the reversed chirality of the systems as evidenced by CD(**1S**)$_{220}$ = 0.932 and CD(**1R**)$_{220}$ = -0.923. Some depression in the signal was observed in the 200 to 210 nm range, however this is a common artefact caused by the sharply increased HT voltage in that range, and the reduced incoming photons from the 500-nm flux of the Xe lamp source.[1]

1. A. Rodger and D. Marshall, *The Biochemist*, 2021, **43**, 58-64.

2. Gelation studies

Gelation was attempted in various solvents, starting at 1.0 wt/v% and adding known amount of the gelator until a gel was formed. A gel was prepared at the lowest necessary concentration for a specific solvent, then additional solvent was added in portions and the gelation repeated until excess solvent was left on top of the gel. The solvent was decanted, the CGC was calculated by weight and a new gel was prepared to confirm the value. The experiment was repeated as necessary.

Table S1. The measured critical gel concentration for MVBTA in various classes of solvents. All values are given as wt/v%.

Group	**Solvent**	**R**	**S**	**R+S**
Polar protic	Methanol	1.7	1.7	1.9
	Ethanol	0.7	0.9	1.4
	n-Propanol	1.2	1.0	2.3
	n-Butanol	1.2	1.0	2.0
	1:1 DMF/H_2O (1:1, v/v)	0.8	0.8	1.2
	1:1 DMSO/H_2O (1:1, v/v)	0.8	0.8	1.3
Polar aprotic	Acetonitrile	0.6	0.6	1.4
	Acetone	1.6	1.6	1.1
	2-Butanone	1.0	1.0	0.8
	Cyclohexanone	1.8	1.9	2.9
	Tetrahydrofuran	2.0	2.0	2.6
	Dioxane	2.3	2.3	4.2
	1,*2*-Dichloroethane	2.7	2.7	4.4
	Chlorobenzene	1.9	2.1	2.9
	Nitrobenzene	0.6	0.7	2.0
Aromatic	Benzene	1.4	1.4	1.3
	Toluene	1.5	1.5	1.2
	o-Xylene	1.2	1.1	0.6
	m-Xylene	1.2	1.1	0.5
	p-Xylene	1.2	1.3	0.5
	Mesitylene	1.2	1.2	0.8

3. Differential Scanning calorimetry (DSC)

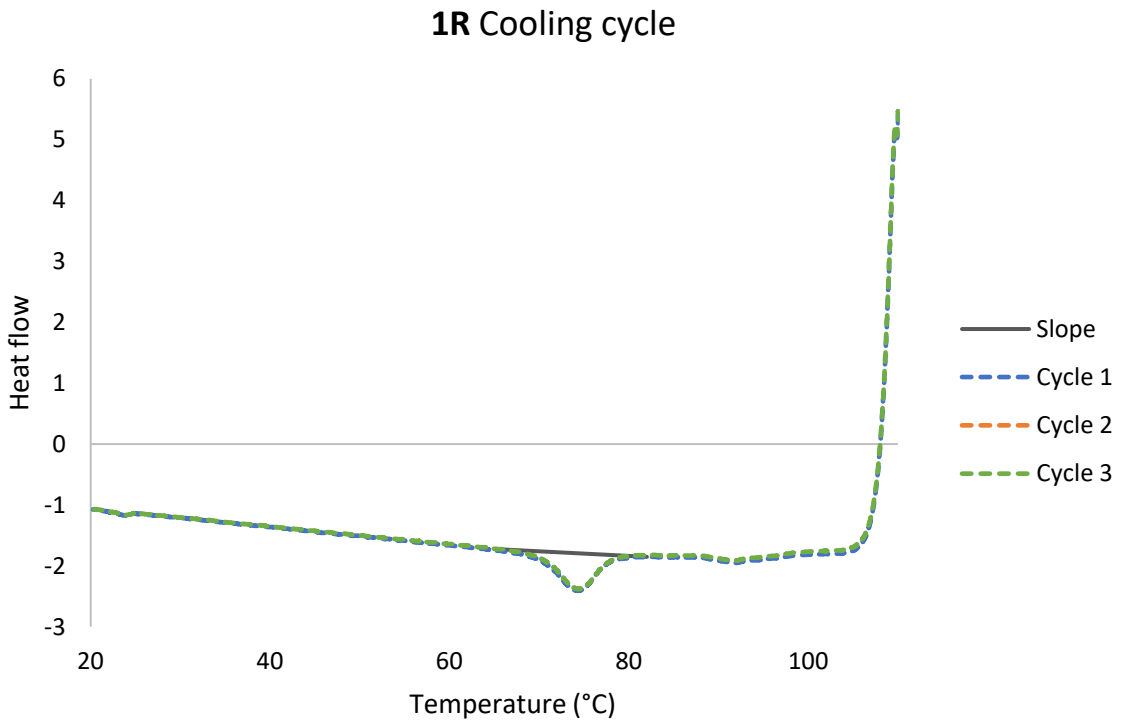

Figure S2. DSC traces showing the cooling cycle of **1R** in *n*-butanol at 2.1 wt/v%, the data overlay each other so the 2nd cycle is not visible.

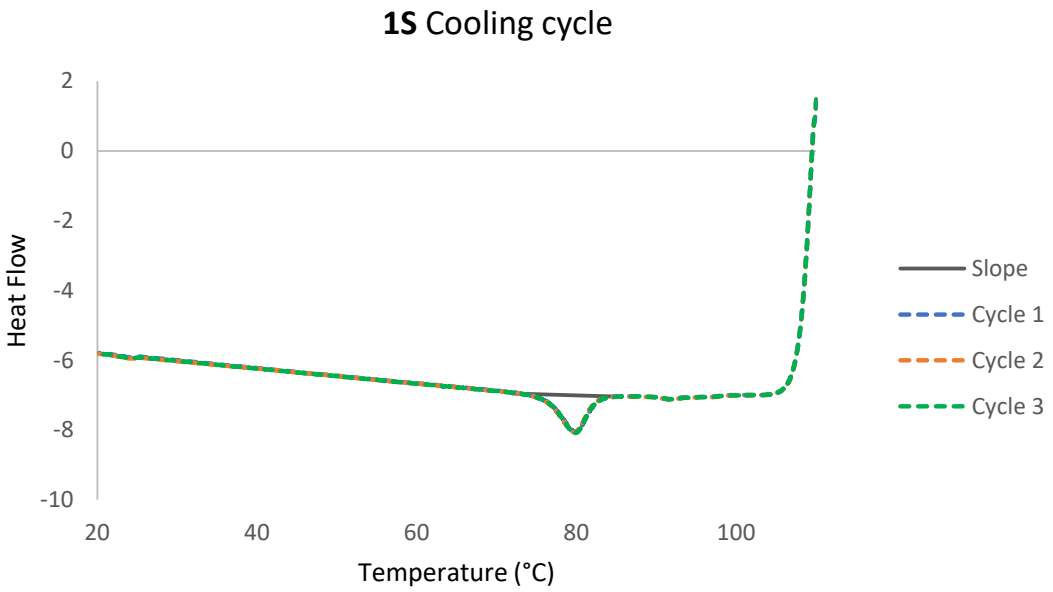

Figure S3. DSC traces showing the cooling cycle of **1S** in *n*-butanol at 2.1 wt/v%, the data overlay each other so the 1st cycle is not visible.

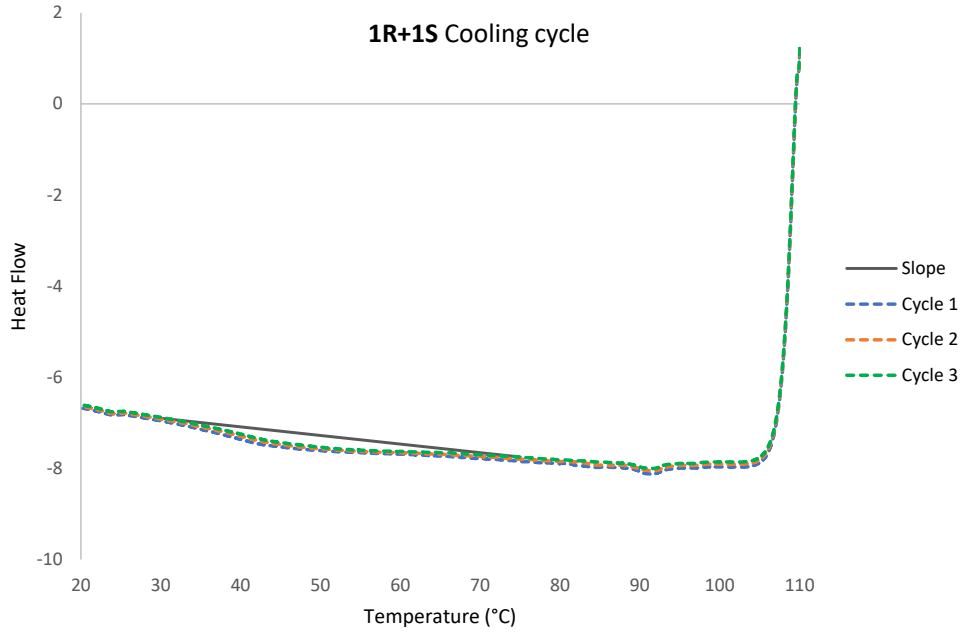

Figure S4. DSC traces showing the cooling cycle of **1R+1S** in *n*-butanol at 2.1 wt/v%.

4. Rheology

The yield stress of the gels was evaluated by amplitude sweep experiments. The results demonstrated that the linear viscoelastic region (LVE) where the gel network undergoes reversible deformation was narrow as the storage modulus G′ declined after 0.02 % of the shear strain **1R**, **1S** and **1R+1S**.

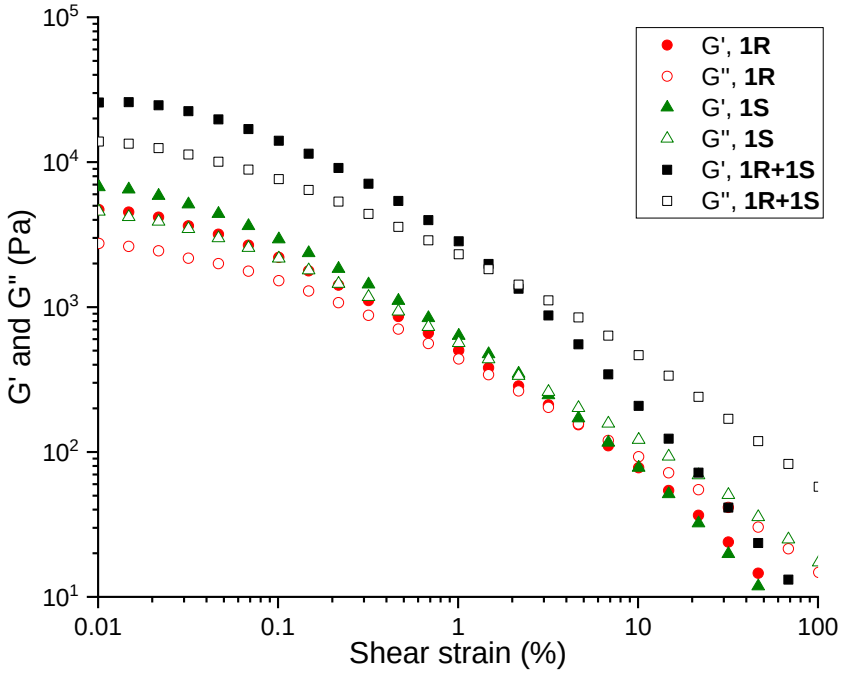

Figure S5. Amplitude sweep measurement performed for **1R**, **1S** and **1R+1S** in MeOH at 3.0 wt/v%.

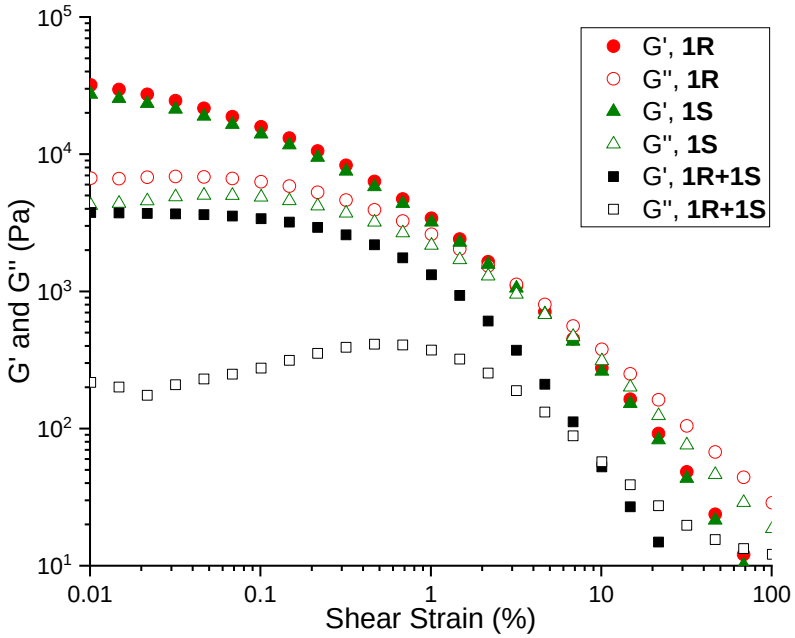

Figure S6. Amplitude sweep measurement performed for **1R**, **1S** and **1R+1S** in 1:1 DMF/H_2O (v/v) at 3.0 wt/v%.

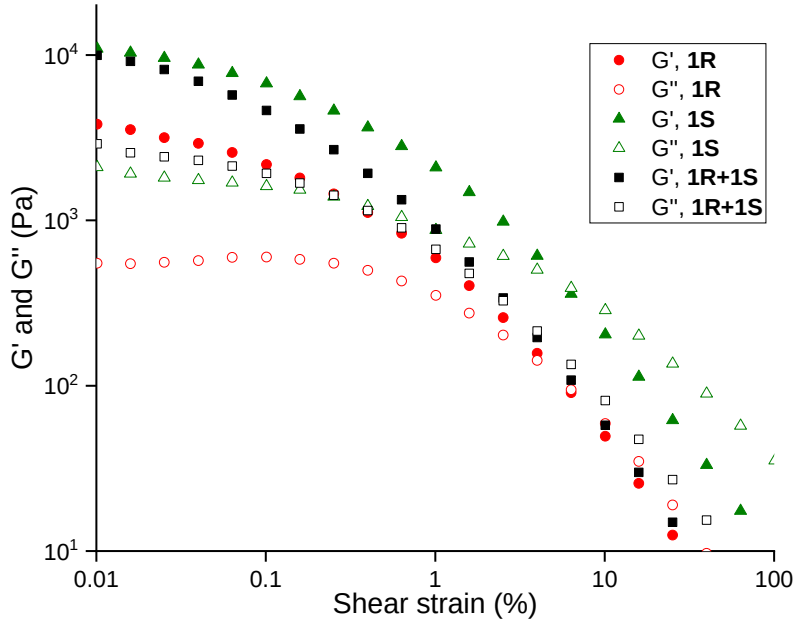

Figure S7. Amplitude sweep measurement performed for **1R**, **1S** and **1R+1S** in mesitylene at 3.0 wt/v%.

Similar results were obtained with toluene, *o*-xylene, toluene, EtOH and DMSO/water (1:1, v/v).

The viscoelastic properties of the gels were evaluated by oscillatory measurements, using a frequency sweep starting at 10 Hz going down to 0.1 Hz with a 0.0125% deformation.

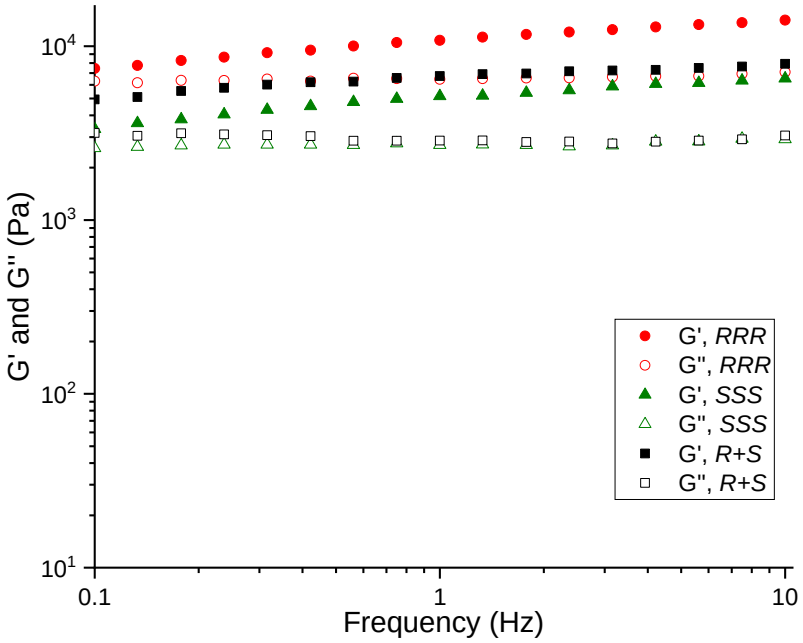

Figure S8. Frequency sweep performed for **1R**, **1S** and **1R+1S** in MeOH at 3.0 wt/v%.

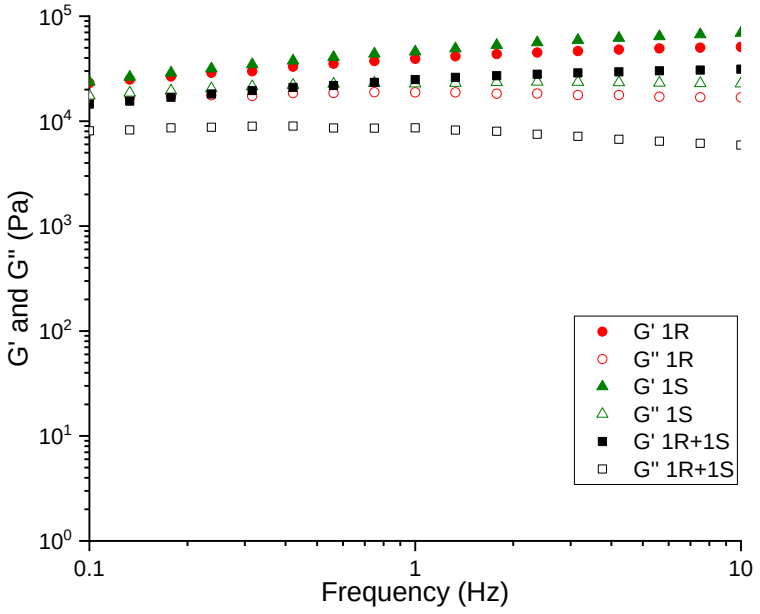

Figure S9. Frequency sweep performed for **1R**, **1S** and **1R+1S** in EtOH at 3.0 wt/v%.

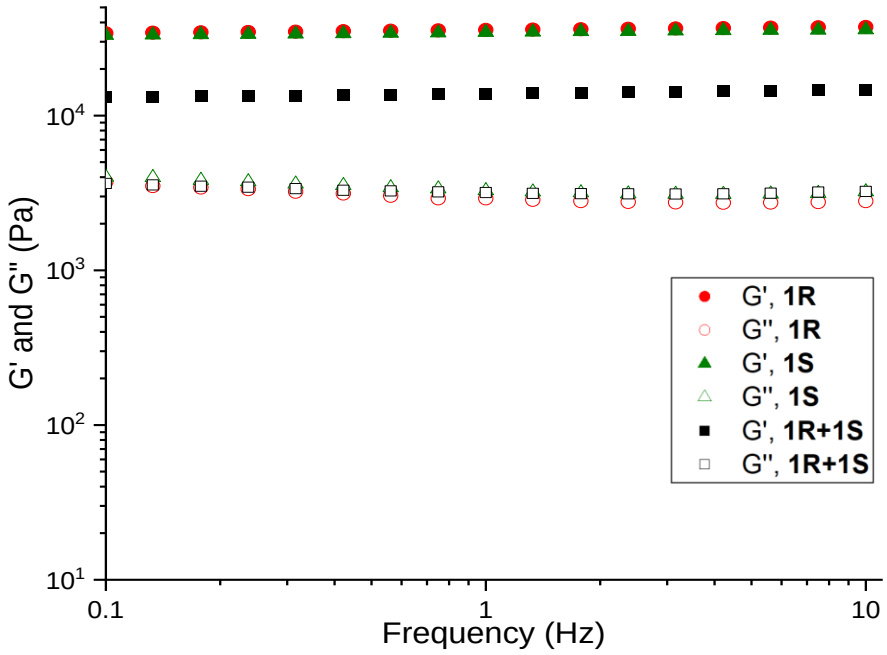

Figure S10. Frequency sweep performed for **1R**, **1S** and **1R+1S** in DMSO/H_2O (1:1, v/v) at 3.0 wt/v%.

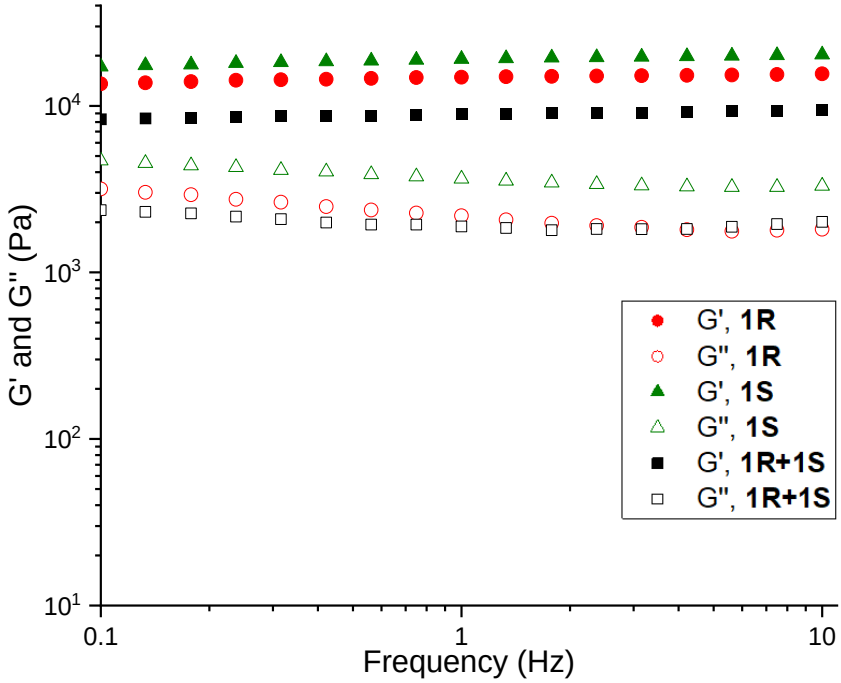

Figure S11. Frequency sweep performed for **1R**, **1S** and **1R+1S** in toluene at 3.0 wt/v%.

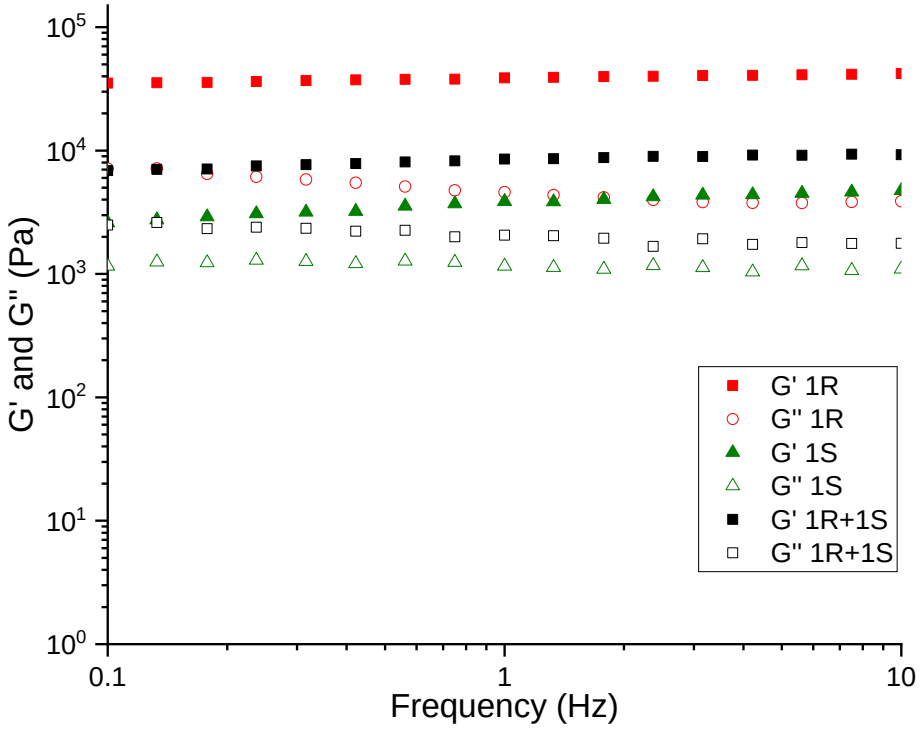

Figure S12. Frequency sweep performed for **1R**, **1S** and **1R+1S** in *o*-xylene at 3.0 wt/v%.

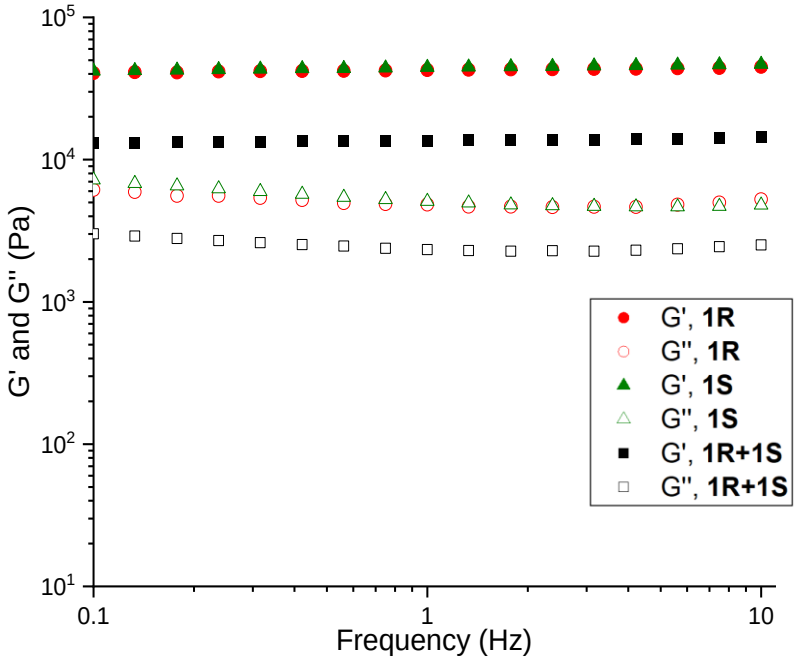

Figure S13. Frequency sweep performed for **1R**, **1S** and **1R+1S** in mesitylene at 3.0 wt/v%.

5. Scanning Electron Microscopy (SEM)

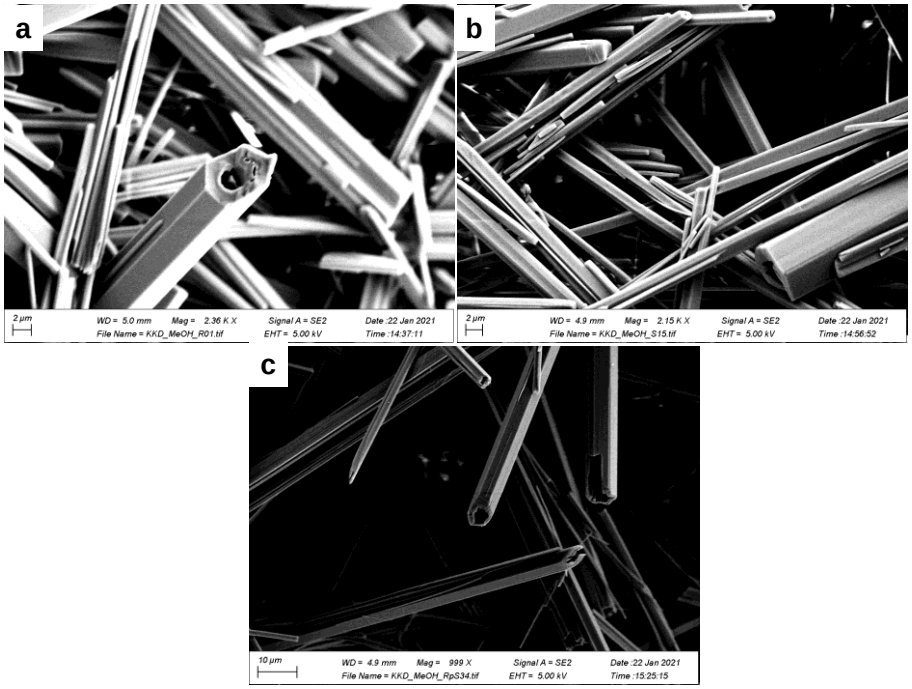

Figure S14. SEM images of a) **1R**, b) **1S** and c) **1R+1S** xerogels from methanol at 2.0 wt/v%.

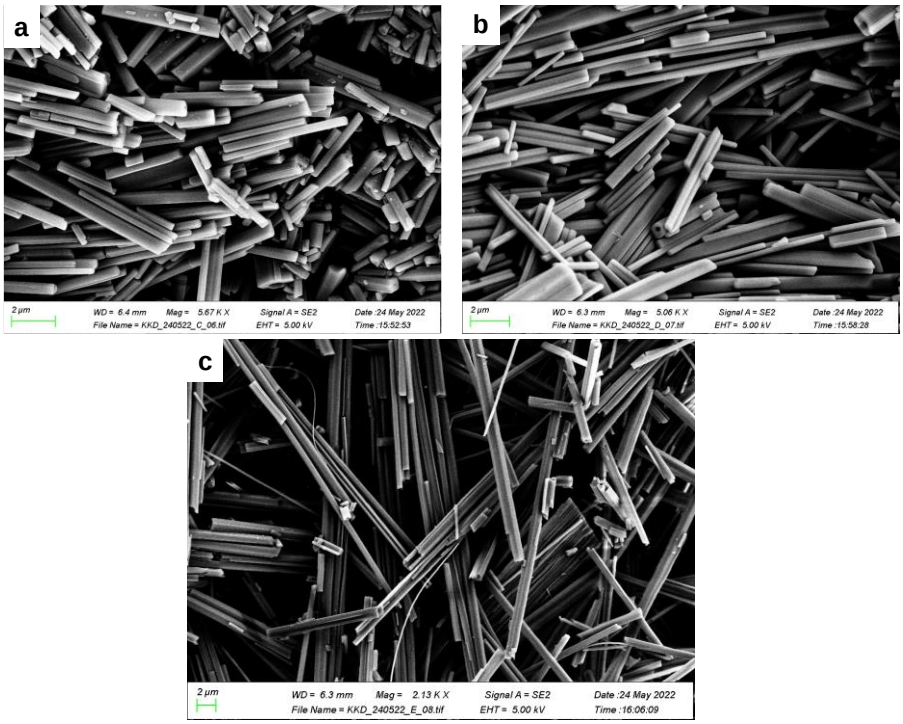

Figure S15. SEM images of a) **1R**, b) **1S** and c) **1R+1S** xerogels generated from gels made in EtOH at 2.0 wt/v%.

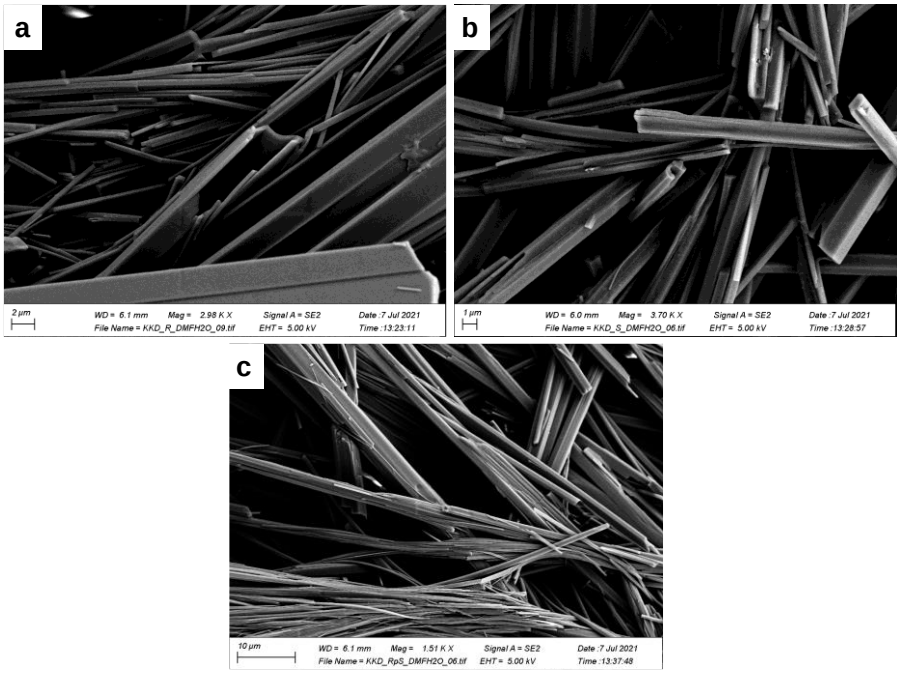

Figure S16. SEM images of a) **1R**, b) **1S** and c) **1R+1S** xerogels generated from gels made in 1:1 DMF/H_2O (v/v) at 2.0 wt/v%.

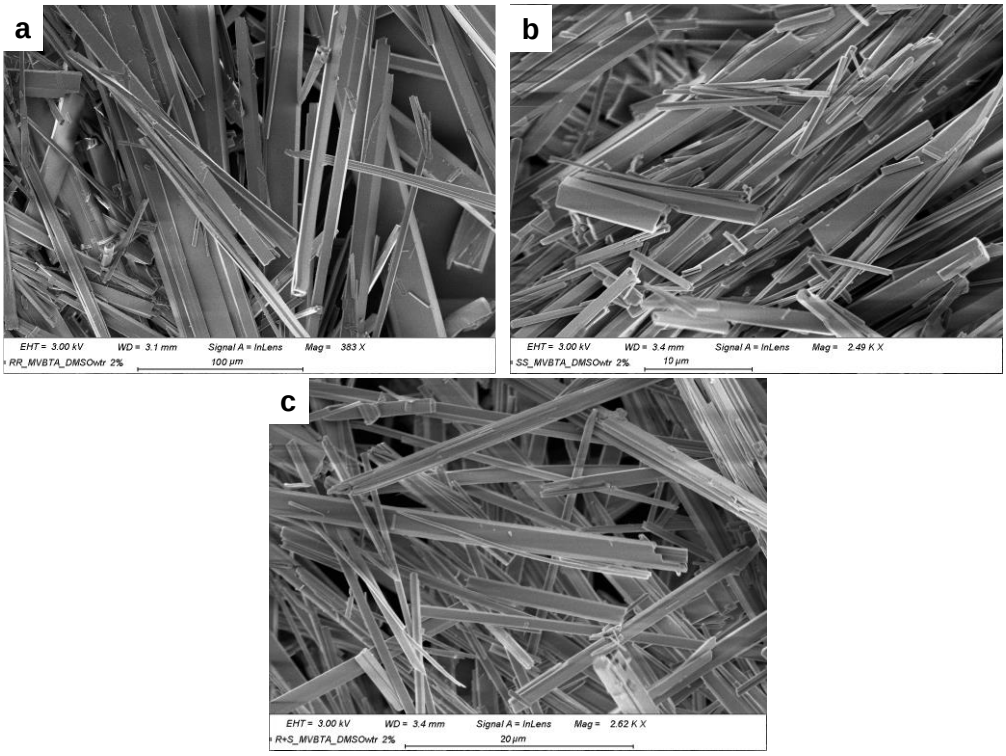

Figure S17. SEM images of a) **1R**, b) **1S** and c) **1R+1S** xerogels generated from gels made in 1:1 DMSO/H_2O (v/v) at 2.0 wt/v%.

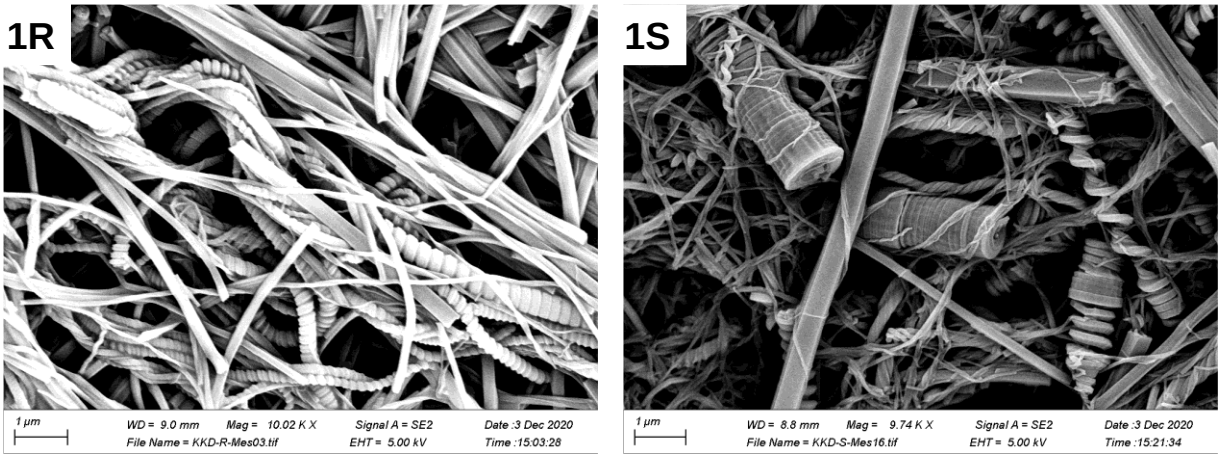

Figure S18. Additional SEM images of enantiomeric xerogels generated from different batches of mesitylene gels at 2.0 wt/v%.

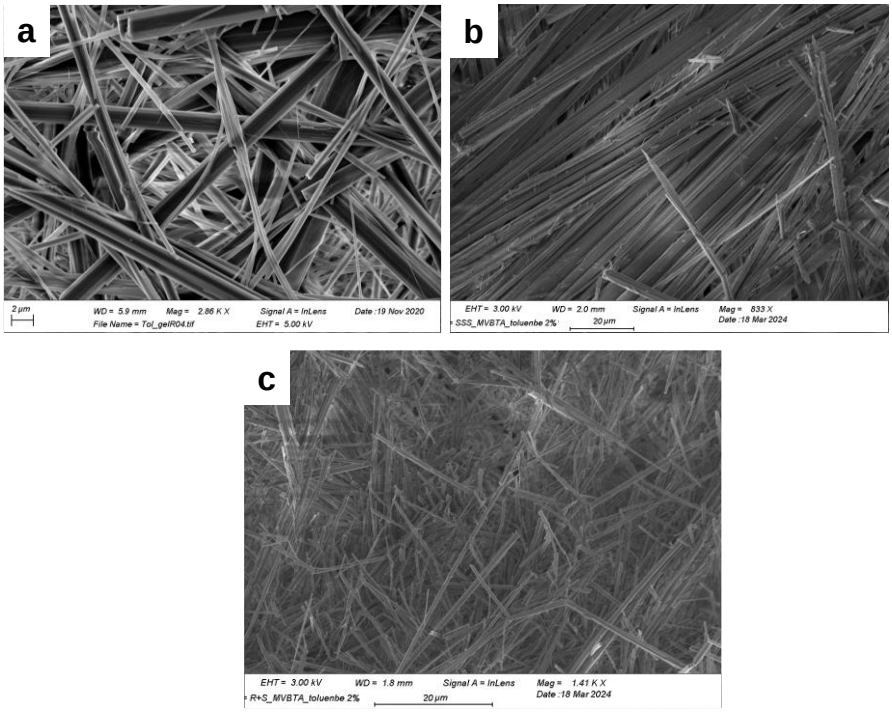

Figure S19. SEM images of a) **1R**, b) **1S** and c) **1R+1S** xerogels from toluene at 2.0 wt/v%.

6. Solid-state ^{13}C-NMR

Solid state NMR spectra were recorded on a Bruker 400 Avance HD with a 3.2 mm HX CP/MAS probe.

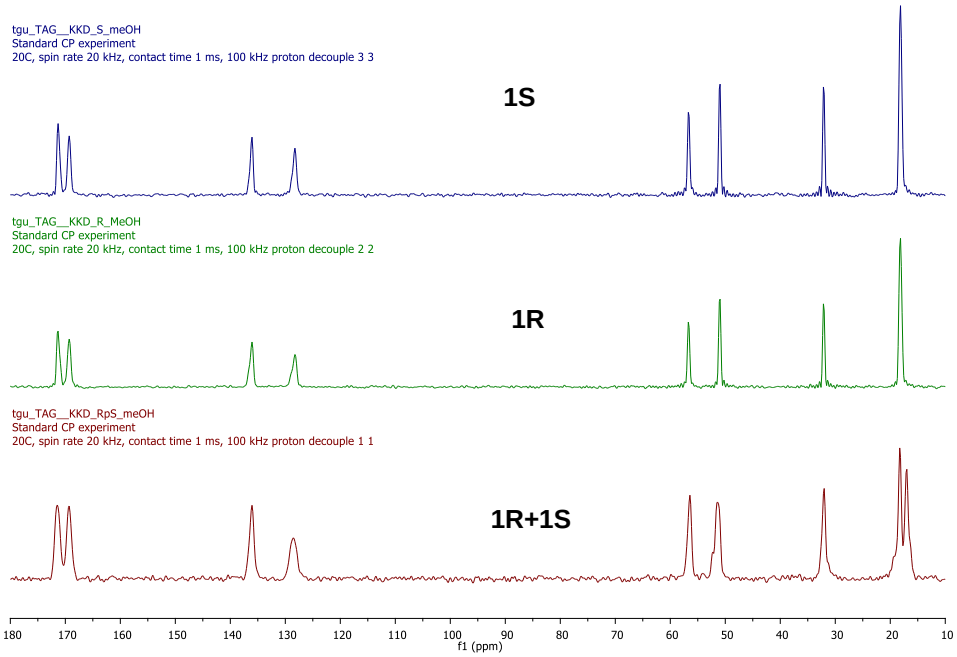

Figure S20: Solid-state ^{13}C-NMR spectra for **1S** (top), **1R** (middle), and **1R+1S** (bottom) xerogels from methanol at 2.0 wt/v%.

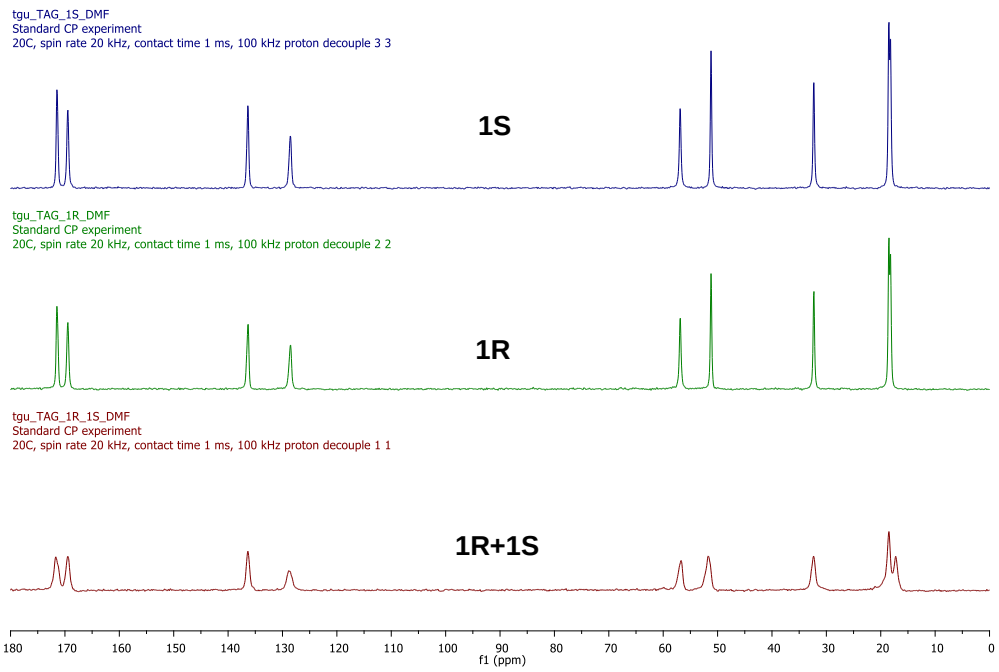

Figure S21. Solid-state ^{13}C-NMR spectra for **1R**, **1S**, and **1R+1S** xerogels in DMF/H_2O (1:1, v/v, polar protic solvent) at 2.0 wt/v%.

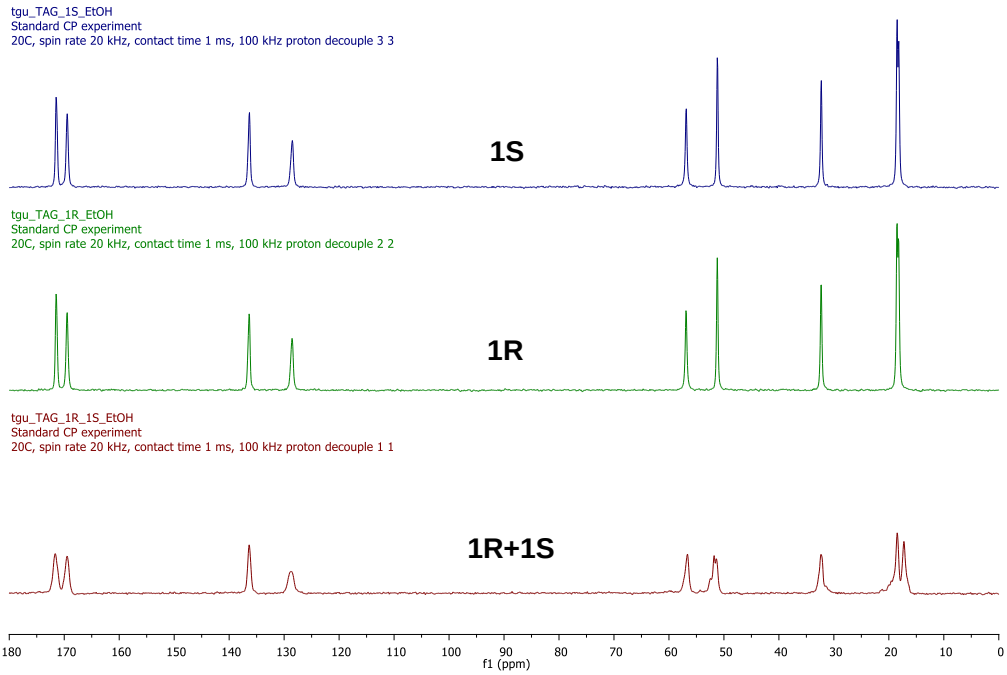

Figure S22. Solid-state ^{13}C-NMR spectra for **1R**, **1S**, and **1R+1S** xerogels in EtOH, (polar protic solvent) at 2.0 wt/v%.

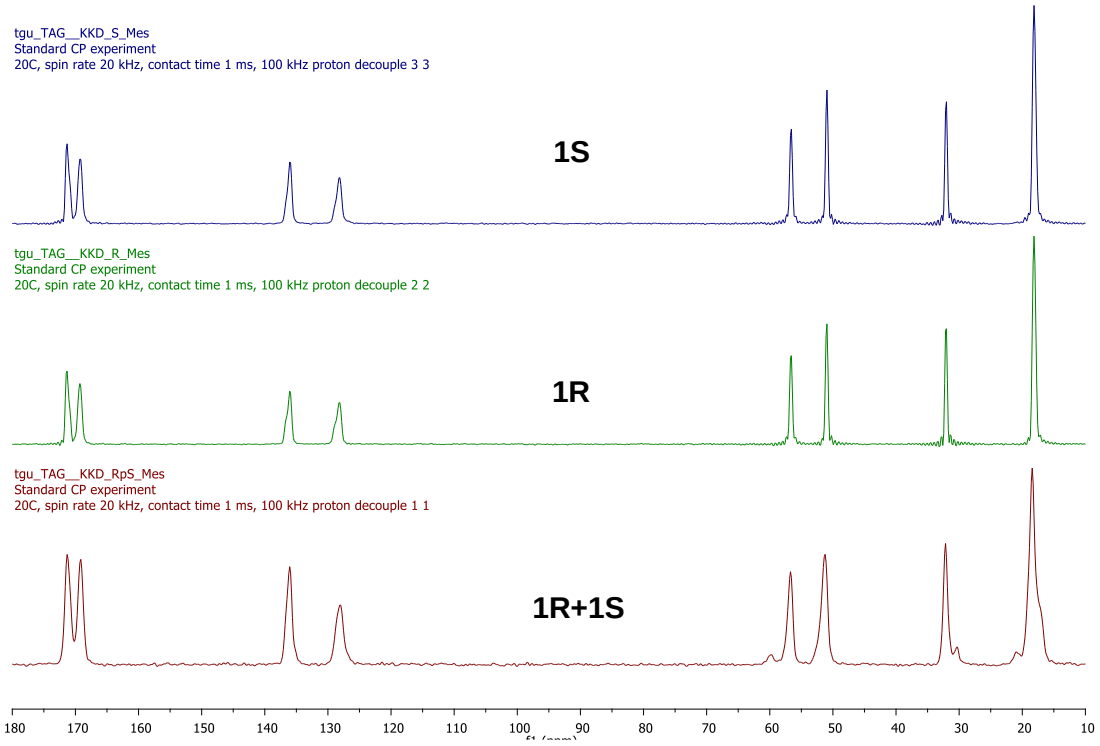

Figure S23. Solid-state ^{13}C-NMR spectra for **1R**, **1S**, and **1R+1S** xerogels in mesitylene (aromatic solvent) at 2.0 wt/v%.

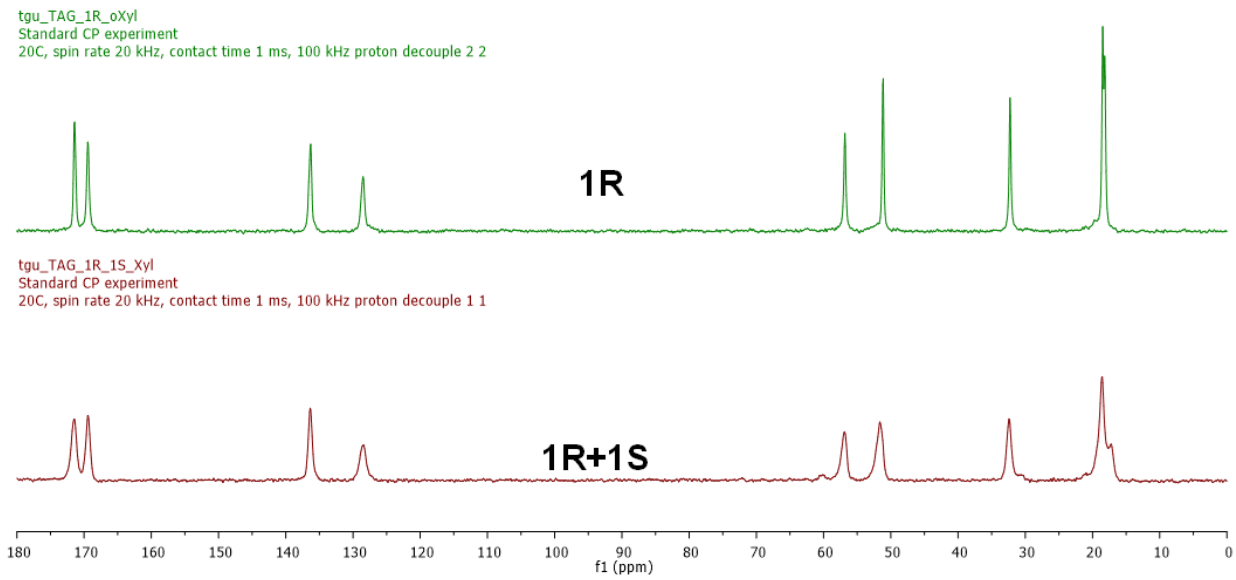

Figure S24. Solid-state ^{13}C-NMR spectra for **1R** and **1R+1S** xerogels in *o*-xylene (aromatic solvent) at 2.0 wt/v%.

7. Powder X-ray Diffraction (PXRD)

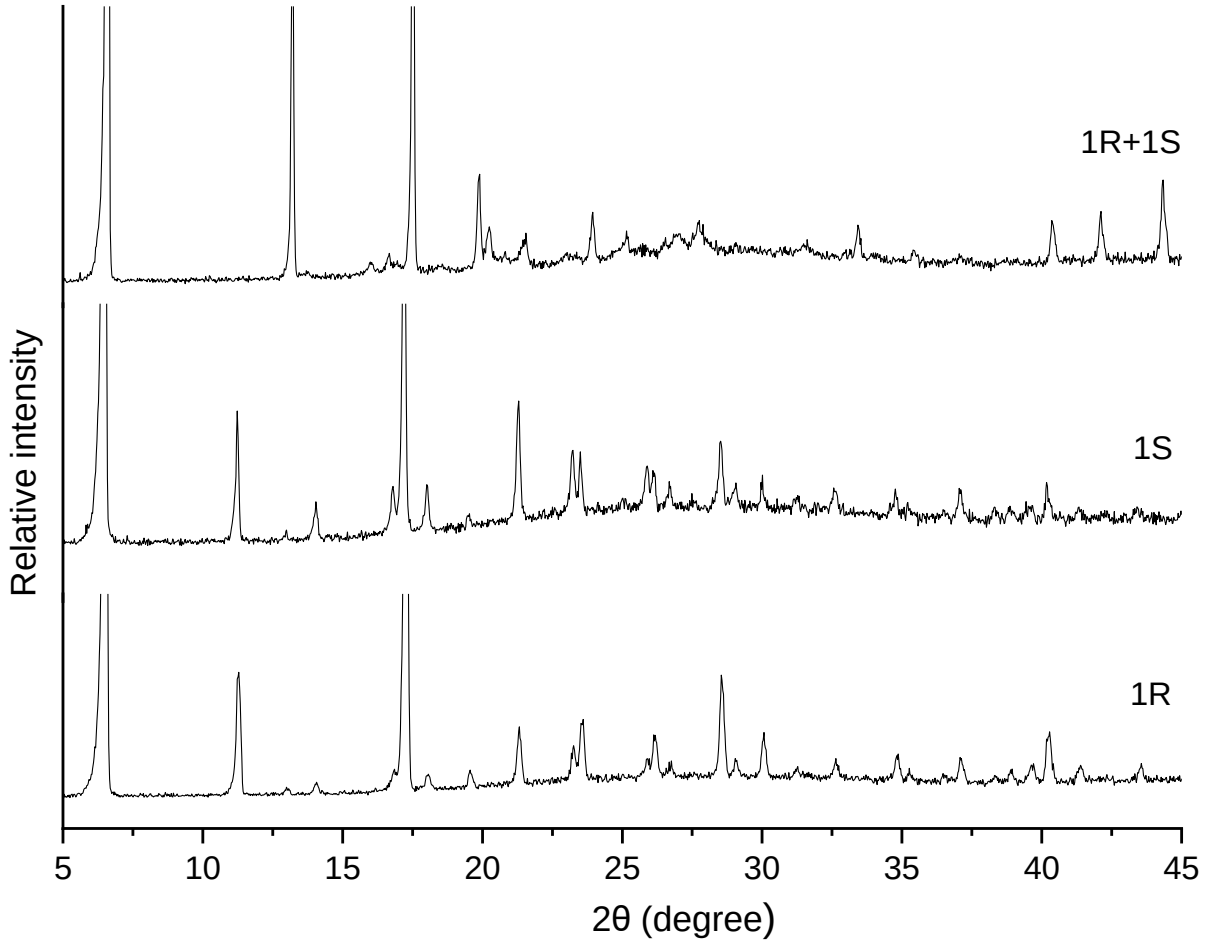

Figure S25. Comparison of PXRD patterns of **1R**, **1S** and **1R+1S** xerogels from methanol (polar protic solvent) at 2.0 wt/v%.

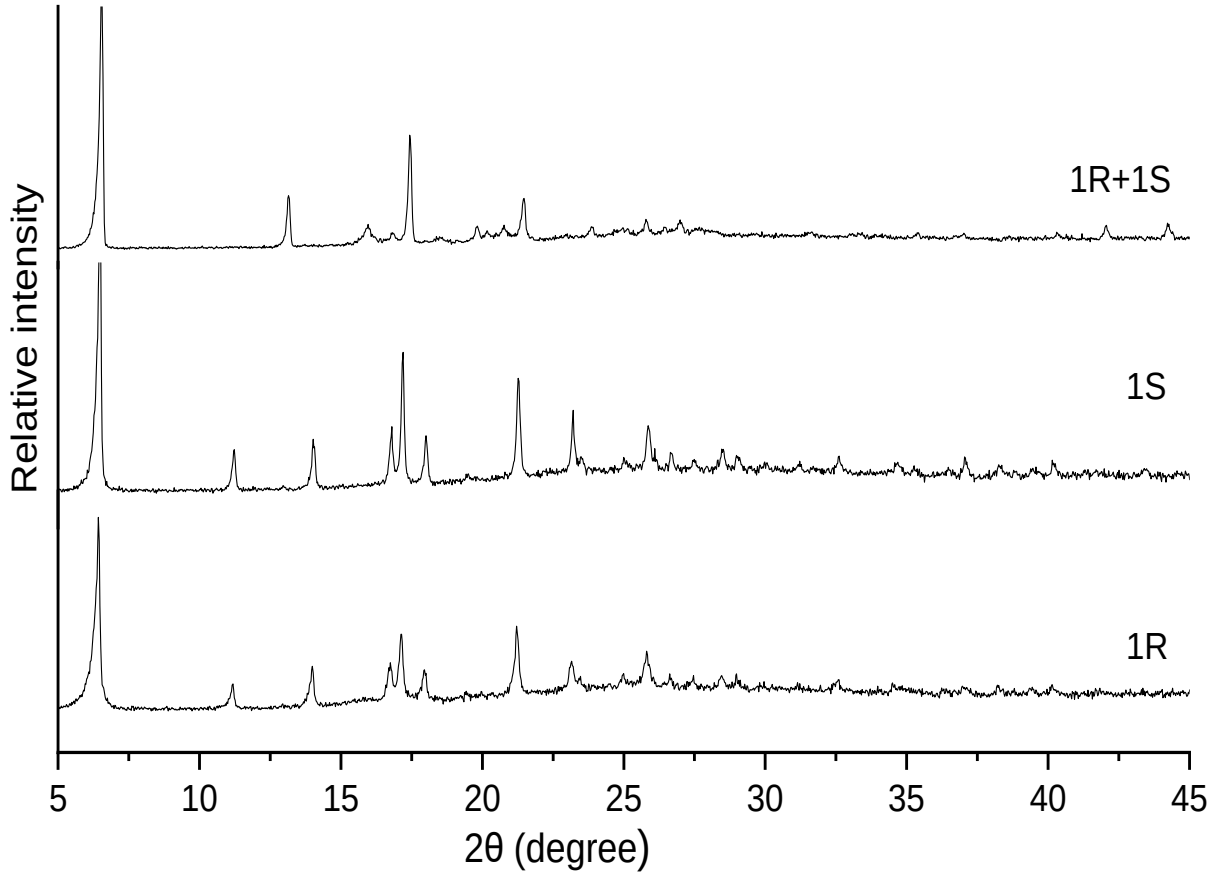

Figure S26. Comparison of PXRD patterns of **1R**, **1S** and **1R+1S** xerogels from ethanol (polar protic solvent) at 2.0 wt/v%.

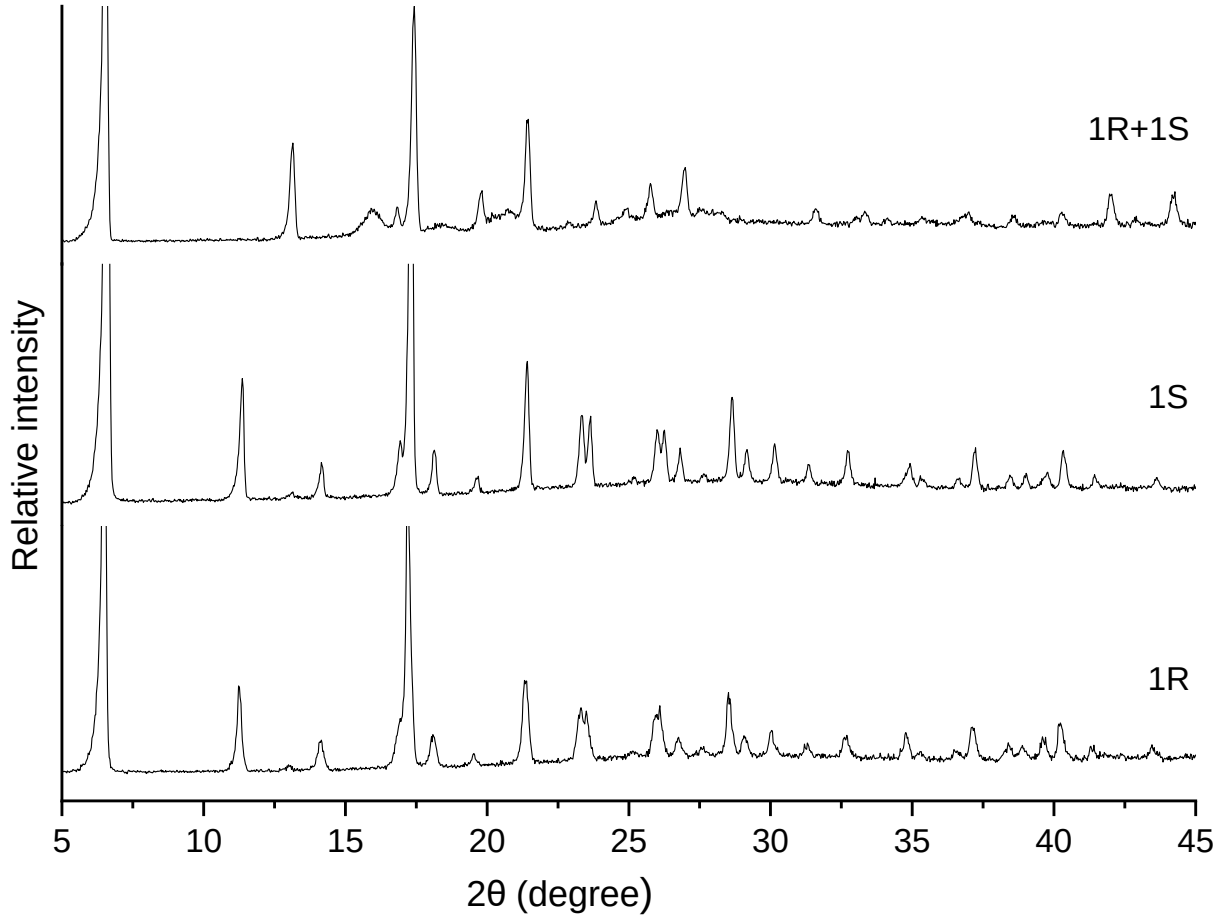

Figure S27. Comparison of XRPD patterns of **1R**, **1S** and **1R+1S** xerogels from DMF/H_2O (1:1, v/v, polar protic solvent) at 2.0 wt/v%.

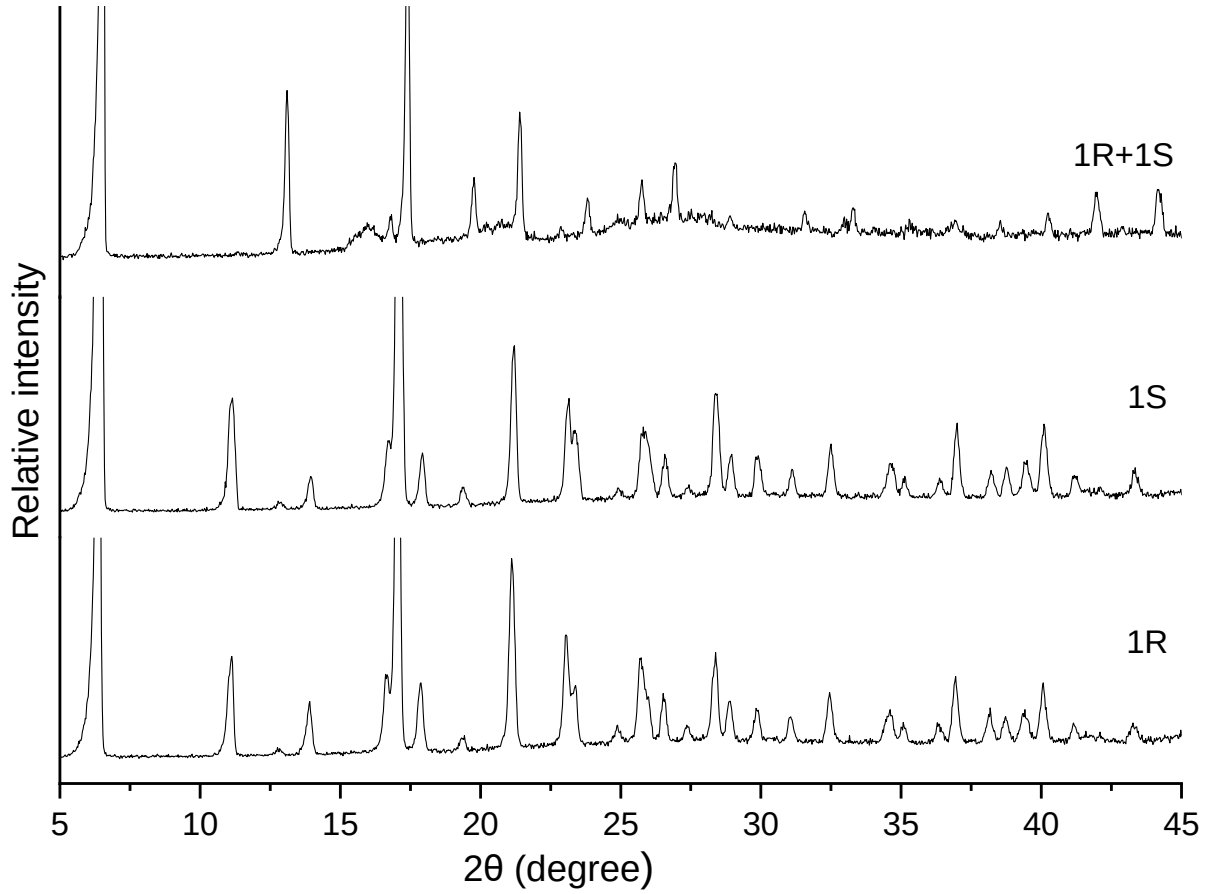

Figure S28. Comparison of XRPD patterns of **1R**, **1S** and **1R+1S** xerogels from DMSO/H_2O (1:1, v/v, polar protic solvent) at 2.0 wt/v%.

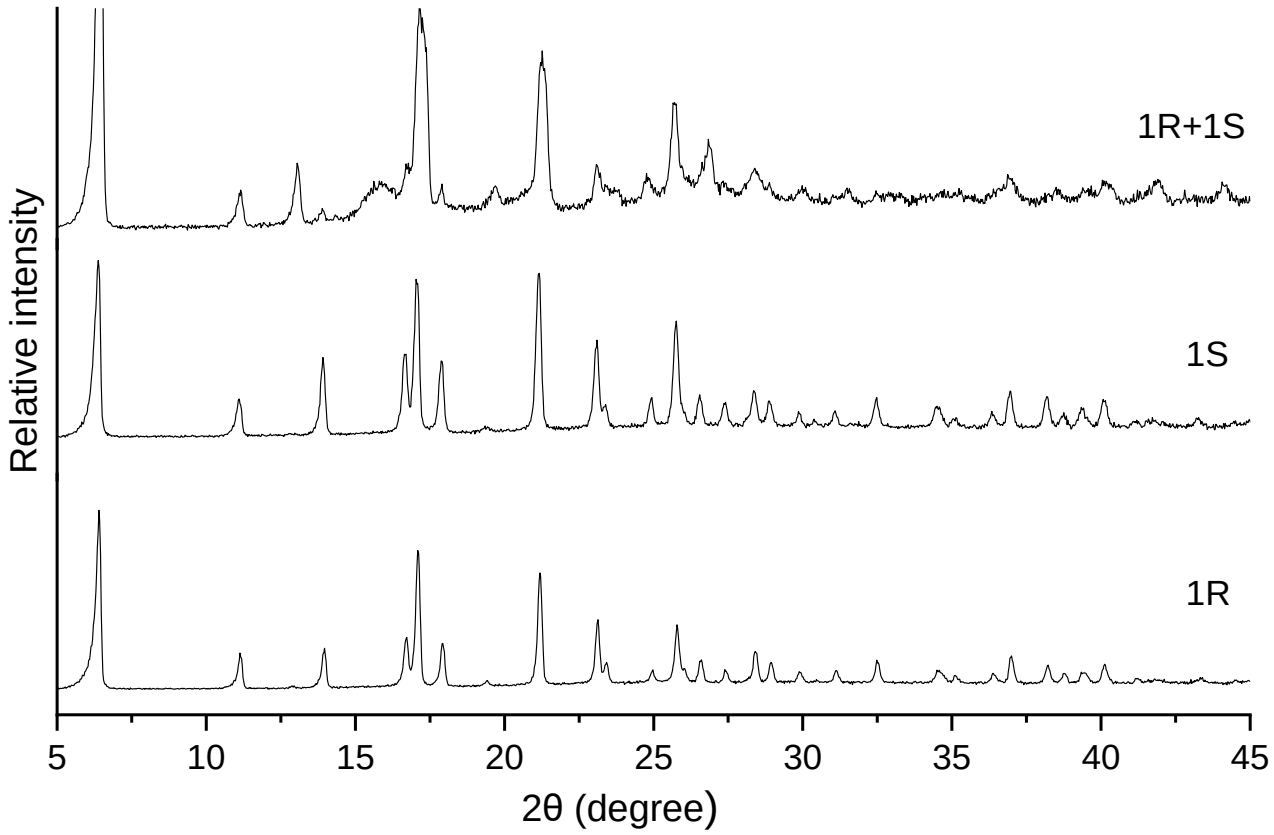

Figure S29. Comparison of XRPD patterns of **1R**, **1S** and **1R+1S** xerogels from *o*-xylene (aromatic solvent) at 2.0 wt/v%.

The mixed gels in *o*-xylene were weakly diffracting but the peaks were matching with toluene and mesitylene.

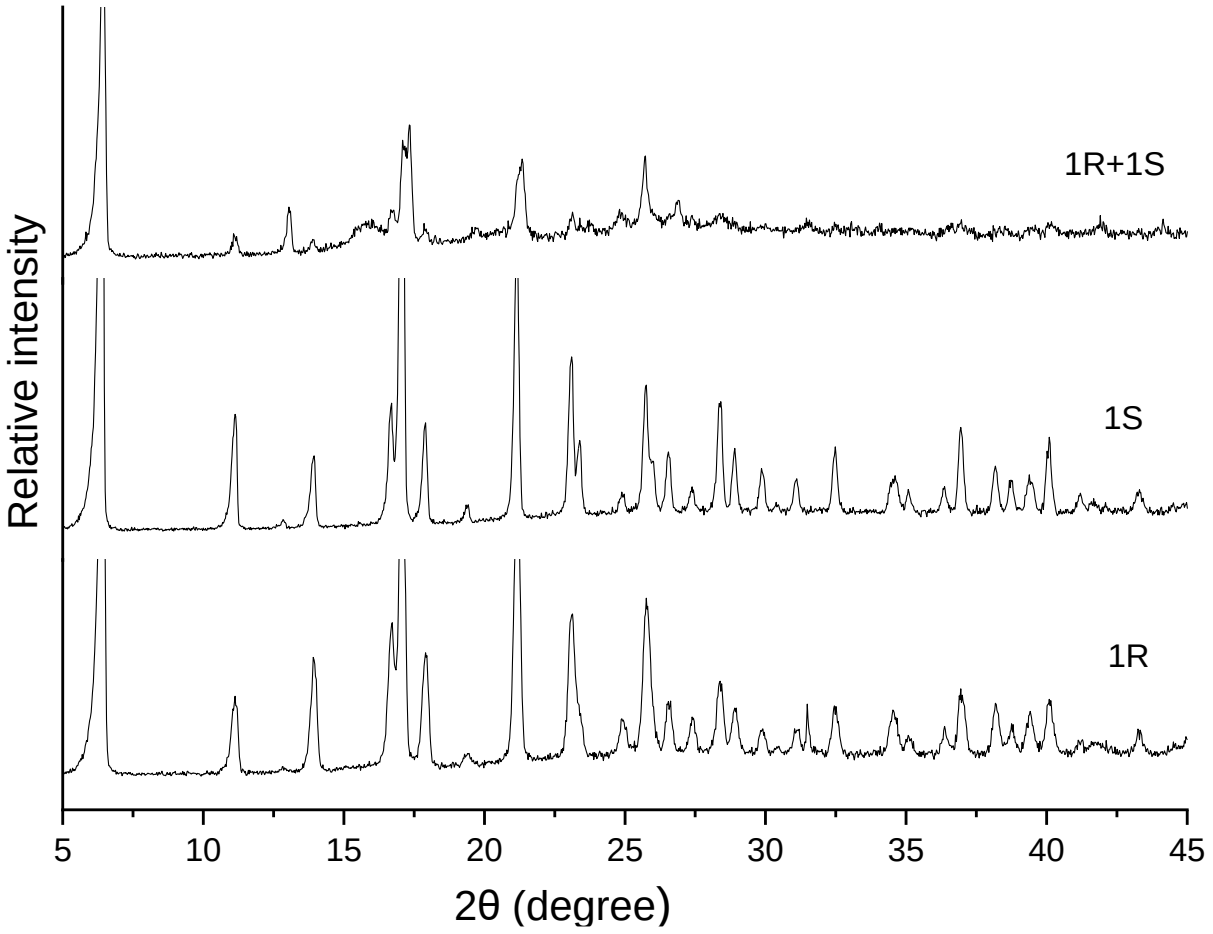

Figure S30. Comparison of XRPD patterns of **1R**, **1S** and **1R+1S** xerogels from toluene (aromatic solvent) at 2.0 wt/v%.

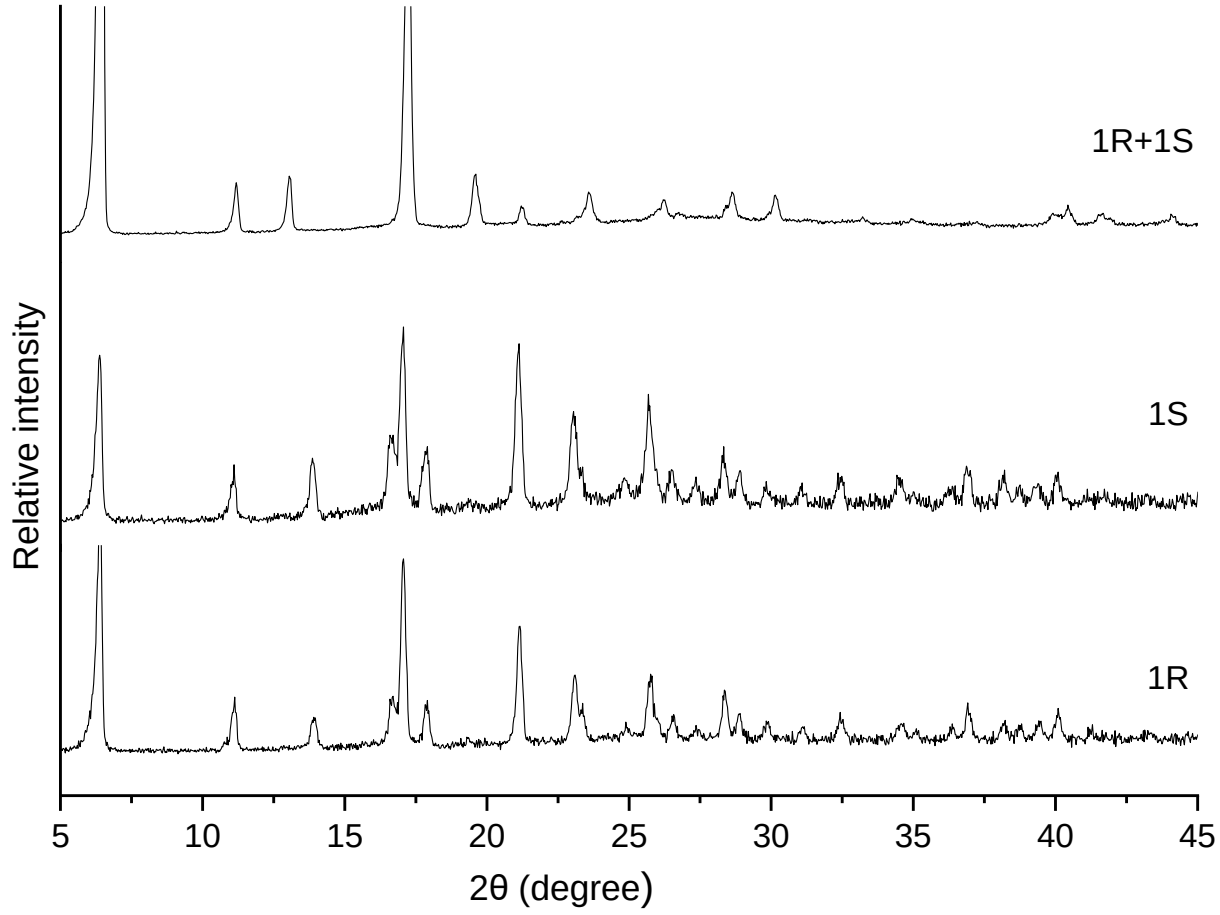

Figure S31. Comparison of XRPD patterns of **1R**, **1S** and **1R+1S** xerogels from mesitylene (aromatic solvent) at 2.0 wt/v%.

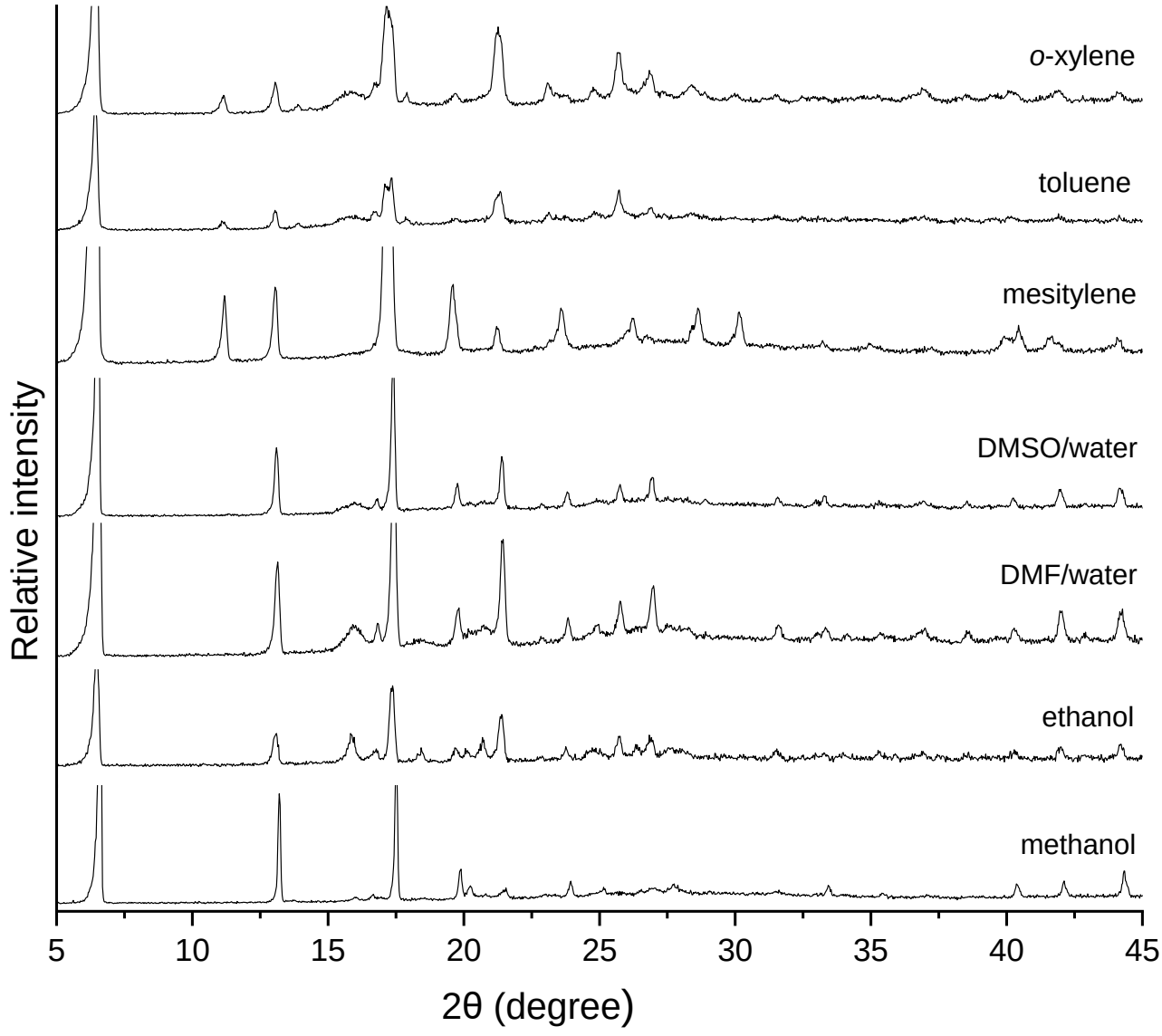

Figure S32. Comparison of XRPD patterns of **1R+1S** xerogels from polar protic solvents (methanol, ethanol, DMF/water (1:1, v/v) and DMSO/water (1:1, v/v) and aromatic solvents (mesitylene, toluene and *o*-xylene).

8. Wide-angle X-ray scattering (WAXS)

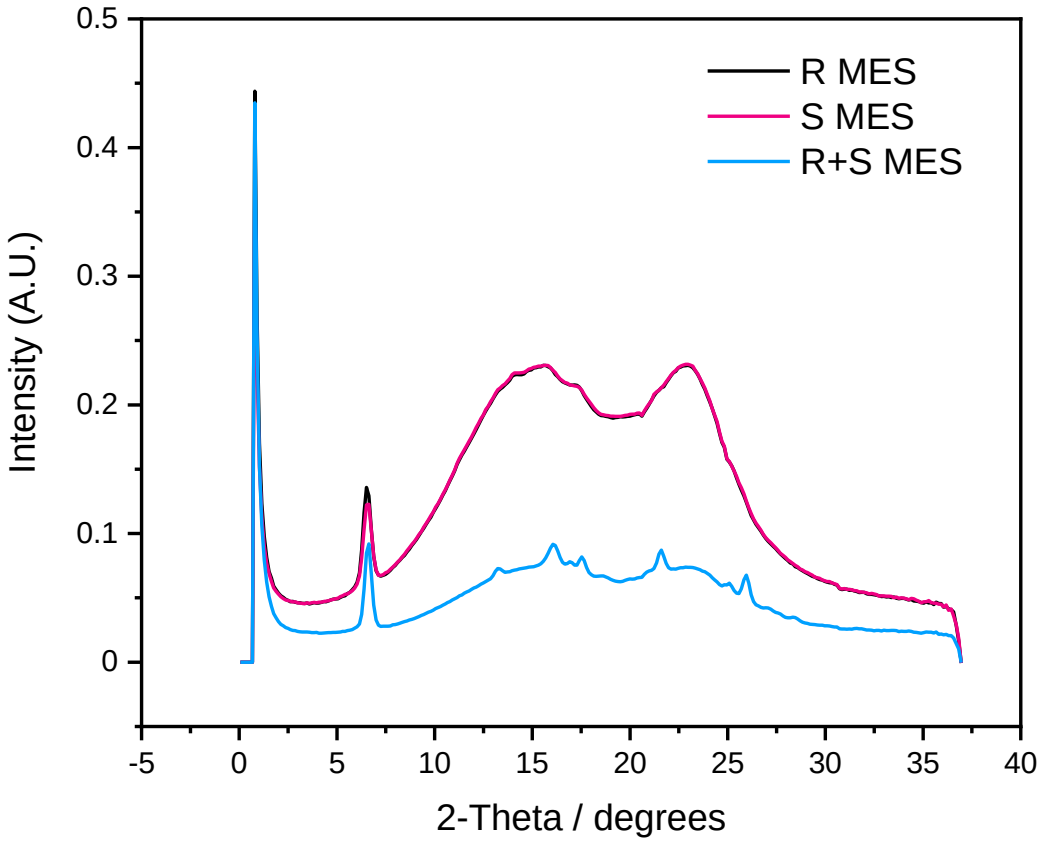

Figure S33. Overlaid WAXS for 2.0 wt/v% MVBTA gels made in mesitylene.

9. Small-angle neutron scattering (SANS)

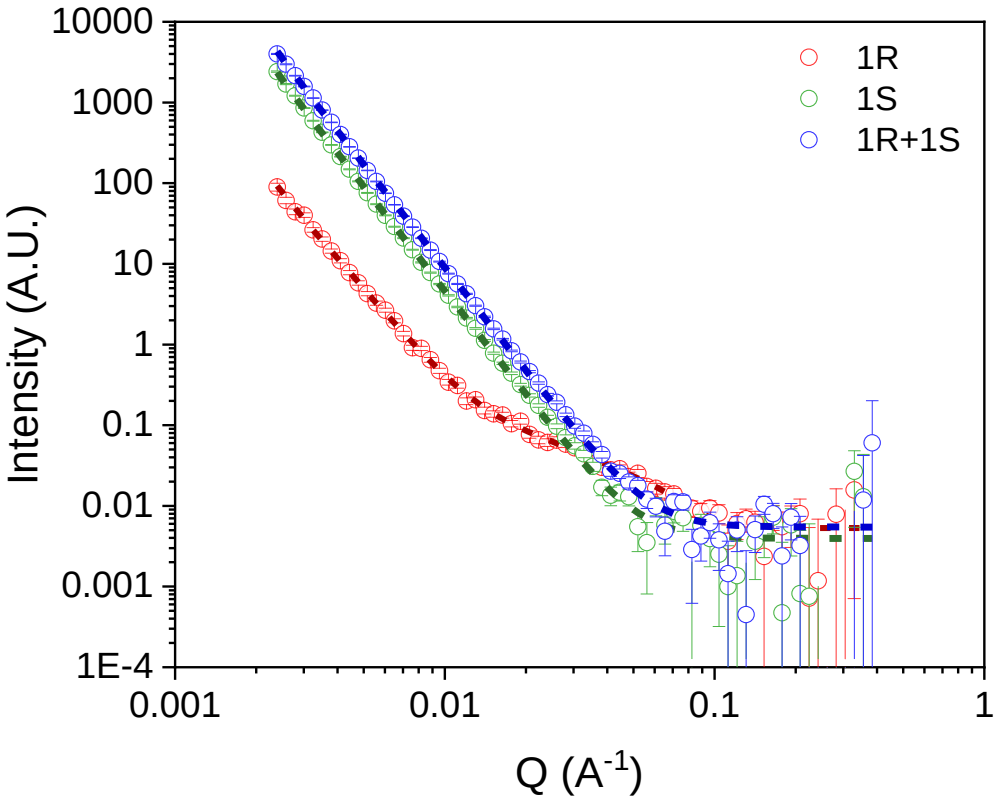

Figure S34. SANS for **1R** (red), **1S** (green), and **1R+1S** (blue) in polar protic solvent (DMSO-d_6/D_2O). In all cases, the fits to the data are shown as broken lines, with the parameters from the fits shown in Table S2.

Table S2. SANS fitting results for MVBTA in polar protic solvent (DMSO-d_6/D_2O).

	1R	**1S**	**1R+1S**
Background / cm^{-1}	0.0053 ± 0.0008	0.0040 ± 0.0005	0.0055 ± 0.0005
Scale	$7.98 \times 10^{-9} \pm 1.97 \times 10^{-10}$	$1.77 \times 10^{-8} \pm 5.28 \times 10^{-10}$	$4.19 \times 10^{-8} \pm 8.63 \times 10^{-10}$
Power Law	3.79 ± 0.04	4.18 ± 0.005	4.14 ± 0.004
Scale (cylinder)	$1.26 \times 10^{-4} \pm 1.93 \times 10^{-5}$		
Radius / Å	28.1 ± 2.5		
Length / A	176 ± 33		
Chi squared	1.2795	2.6988	4.9541

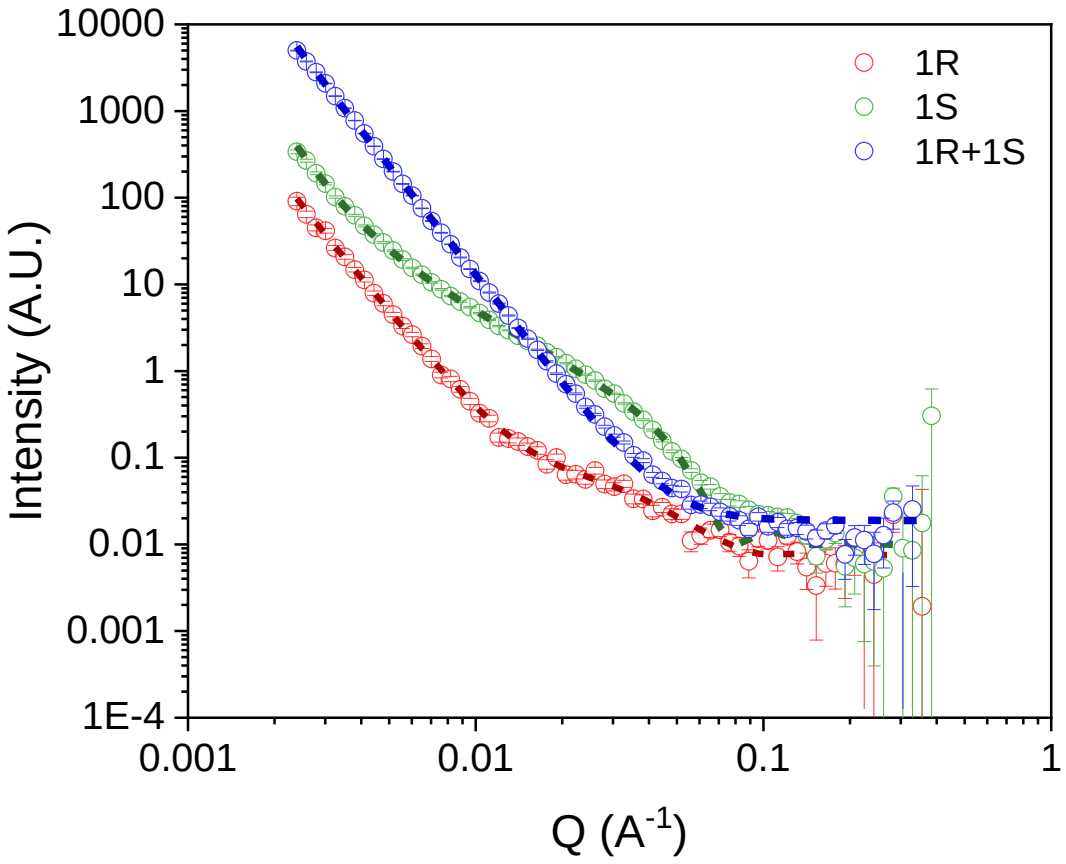

Figure S35. SANS for **1R** (red), **1S** (green), and **1R+1S** (blue) in aromatic solvent, toluene-d_8). In all cases, the fits to the data are shown as broken lines, with the parameters from the fits shown in Table S3.

Table S3. SANS fitting results for MVBTA in aromatic solvent (toluene-d_8).

	1R	**1S**	**1R+1S**
Background / cm^{-1}	0.0075 ± 0.0007	0.0021 ± 0.0008	0.016 ± 0.0006
Scale	$5.97 \times 10^{-9} \pm 1.33 \times 10^{-10}$	$4.44 \times 10^{-7} \pm 1.1 \times 10^{-9}$	$8.40 \times 10^{-8} \pm 1.45 \times 10^{-9}$
Power Law	3.79 ± 0.04	4.48± 0.04	4.07 ± 0.003
Scale (flexible cylinder)	$8.46 \times 10^{-5} \pm 1.16 \times 10^{-7}$	$7.88 \times 10^{-4} \pm 7.37 \times 10^{-5}$	
Radius / Å	31.5 ± 3.8	47.4 ± 0.3	
Length / A	133 ± 21	5000*	
Kuhn Length / A		141 ± 3	
Chi squared	1.333	7.743	10.463

* Fixed value